ORIGINAL ARTICLE

Cytoplasmic poly-GA aggregates impair nuclear import of TDP-43 in *C9orf72* ALS/FTLD

Bahram Khosravi[1,2,†], Hannelore Hartmann[1,†], Stephanie May[1], Christoph Möhl[3], Helena Ederle[2,4], Meike Michaelsen[1], Martin H. Schludi[1,5], Dorothee Dormann[2,4] and Dieter Edbauer[1,2,5,*]

[1]German Center for Neurodegenerative Diseases (DZNE), Munich, Feodor-Lynen-Str. 17, 81377 Munich, Germany, [2]Graduate School of Systemic Neuroscience (GSN), Ludwig-Maximilians-University Munich, Germany, [3]Image and Data Analysis Facility, German Center for Neurodegenerative Diseases (DZNE), Bonn, Ludwig-Erhard-Allee 2, 53175 Bonn, Germany, [4]Biomedical Center (BMC), Institute for Cell Biology (Anatomy III), Ludwig Maximilians University Munich, Großhaderner Strasse 9, 82152 Planegg-Martinsried, Germany and [5]Munich Cluster of Systems Neurology (SyNergy), Feodor-Lynen-Str. 17, 81377 Munich, Germany

*To whomcorrespondence should be addressed at: DZNE, Feodor-Lynen-Str. 17, 81377 Munich, Germany. Tel: +4989440046510; Fax: +4989440046508; Email: dieter.edbauer@dzne.de

Abstract

A repeat expansion in the non-coding region of *C9orf72* gene is the most common mutation causing frontotemporal lobar degeneration (FTLD) and amyotrophic lateral sclerosis (ALS). Sense and antisense transcripts are translated into aggregating dipeptide repeat (DPR) proteins in all reading frames (poly-GA,-GP,-GR,-PA and -PR) through an unconventional mechanism. How these changes contribute to cytoplasmic mislocalization and aggregation of TDP-43 and thereby ultimately leading to neuron loss remains unclear. The repeat RNA itself and poly-GR/PR have been linked to impaired nucleocytoplasmic transport. Here, we show that compact cytoplasmic poly-GA aggregates impair nuclear import of a reporter containing the TDP-43 nuclear localization (NLS) signal. However, a reporter containing a non-classical PY-NLS was not affected. Moreover, poly-GA expression prevents TNFα induced nuclear translocation of p65 suggesting that poly-GA predominantly impairs the importin-α/β-dependent pathway. In neurons, prolonged poly-GA expression induces partial mislocalization of TDP-43 into cytoplasmic granules. Rerouting poly-GA to the nucleus prevented TDP-43 mislocalization, suggesting a cytoplasmic mechanism. In rescue experiments, expression of importin-α (KPNA3, KPNA4) or nucleoporins (NUP54, NUP62) restores the nuclear localization of the TDP reporter. Taken together, inhibition of nuclear import of TDP-43 by cytoplasmic poly-GA inclusions causally links the two main aggregating proteins in *C9orf72* ALS/FTLD pathogenesis.

Introduction

Amyotrophic lateral sclerosis (ALS) and frontotemporal lobar degeneration (FTLD) are two devastating neurodegenerative diseases with overlapping pathology and genetics (1). The pathogenic *C9orf72* repeat expansion is the most common genetic cause of ALS and FTLD. Upon autopsy, *C9orf72* patients present typical cytoplasmic TDP-43 aggregates that are also seen in other familial and sporadic ALS/FTLD cases (2). Three potential pathomechanisms leading to *C9orf72* ALS/FTLD have been proposed so far. Reduced expression from the mutant *C9orf72* allele may inhibit autophagy and promote neuroinflammation without causing overt neurodegeneration by itself (3–5). The RNA containing hundreds or thousands GGGGCC repeats rather than 2–30 repeats seen in healthy people is thought to sequester a number of RNA-binding proteins in nuclear RNA foci (6). Repeat-associated non-ATG translation (7) of the intronic repeat in all reading frames gives rise to five dipeptide repeat (DPR) proteins. The sense transcript-derived poly-GA, poly-GR and poly-GP are much more abundant than poly-PA and poly-PR derived from the antisense transcript (8–11). The DPR proteins coaggregate in compact inclusions predominantly in the cytoplasm of neurons in the neocortex, cerebellum and thalamus. In patients DPR inclusions likely appear several years prior to TDP-43 pathology (12). TDP-43 pathology correlates better with regional neurodegeneration than DPR pathology (13) and DPR and TDP-43 inclusions appear mostly in distinct cells. If they occur in the same cell, TDP-43 seems to coat the poly-GA aggregates (8). Intercellular spreading of both aggregated poly-GA (14,15) and TDP-43 (16) has been reported.

The cause of TDP-43 aggregation in *C9orf72* ALS/FTLD is still largely unclear (17). We and others have found no obvious effect on TDP-43 upon expression of individual DPR proteins in cell lines (18–21). High level expression of (GGGGCC)$_{66}$ using AAV results in significant TDP-43 aggregation and neurodegeneration, although the TDP-43 inclusions are (unlike in patients) predominantly found within the nucleus (22). Several BAC-transgenic lines replicate DPR and RNA foci pathology (4,23,24), but strangely only one such line additionally showed TDP-43 inclusions and rapid neurodegeneration in a subset of female animals (25).

Recently, several groups have reported impaired nucleocytoplasmic transport in several *C9orf72* models and attributed it to the repeat RNA (26), poly-GR/PR (27) or both (28). The repeat RNA or poly-GR/PR are thought to disrupt the nucleocytoplasmic Ran-GTP gradient that is crucial for correct sorting of most proteins, but the mechanism remains unclear (29). Similarly, altered RanGAP1 localization has been reported in mice with high levels of poly-GA expression, but the functional consequences have not been addressed (30). Recently, it was shown that artificial aggregating β-sheet proteins impair nucleocytoplasmic transport due to sequestration of the THOC complex and RNA binding proteins (31). Since GA$_{15}$ peptides also form typical amyloid fibrils (14) we speculated that poly-GA may also impair nucleocytoplasmic transport.

Therefore, we tested whether poly-GA, poly-GR and poly-PR affect the nuclear import of TDP-43, because cytoplasmic TDP-43 aggregation may ultimately trigger neurodegeneration in *C9orf72* cases. We analysed cytoplasmic mislocalization of endogenous TDP-43 and of a reporter containing the bipartite classical nuclear localization signal (NLS) of TDP-43. This signal has been shown to mediate TDP-43 nuclear import of TDP-43 via the importin-α/β pathway (32–34). To elucidate the mechanism of impaired nuclear import of TDP-43, we redirected the cytoplasmic poly-GA aggregates into the nucleus and performed rescue experiments using key components of the nuclear import machinery.

Results

Poly-GA causes mislocalization of a TDP-43 NLS reporter

To test functional consequences of DPR expression on nucleocytoplasmic transport of TDP-43 in HeLa cells, we generated a fluorescence-based reporter containing RFP fused with the nuclear localization signal (NLS) of TDP-43, a well characterised bipartite NLS (33). Upon co-expression of RFP-NLS$_{TDP}$ with GFP, RFP-NLS$_{TDP}$ almost exclusively localised to the nucleus in HeLa cells in interphase, as expected (Fig. 1A first row). In contrast, many cells with GA$_{149}$-GFP inclusions showed significant levels of the RFP-reporter in the cytoplasm suggesting impaired nuclear import mediated by this classical NLS (Fig. 1A, second row, arrows). Quantitative analysis using manual counting confirmed significant mislocalization of the reporter in ~40% of inclusion bearing cells compared to ~5% of GFP expressing cells (Fig.1B). In contrast, only about 20% of cells with compact GFP-GR$_{149}$ or PR$_{175}$-GFP inclusions showed enhanced cytoplasmic RFP-NLS$_{TDP}$ localization (Fig. 1A, third and fourth row). While GA$_{149}$-GFP and GFP-GR$_{149}$ were expressed at a similar level, the weaker effect of poly-PR may be due to the lower expression of PR$_{175}$-GFP (Supplementary Material, Fig. S1A). Using automated image analysis with the Columbus Acapella system, we confirmed mislocalization of the RFP-NLS$_{TDP}$ reporter in poly-GA expressing cells by comparing the mean cytoplasmic RFP fluorescence in double transfected cells (Fig. 1C). Moreover, we used differential centrifugation to separate the cytosolic and nuclear fraction of the RFP-NLS$_{TDP}$ reporter in DPR expressing cells. As expected, the majority of RFP-NLS$_{TDP}$ was in the histone 3 positive nuclear fraction. However, the cytosolic fraction of RFP-NLS$_{TDP}$ was increased in the GA$_{149}$-GFP cotransfected HeLa cells (Fig. 2A and B). Immunostaining revealed no cytoplasmic mislocalization of endogenous TDP-43 in GFP-DPR expressing HeLa cells 2 days after transfection (data not shown).

While importin-α/β recognises the NLS of TDP-43, transportin (TNPO) binds to so-called PY-NLS motifs to initiate the nuclear import of other proteins, such as hnRNPA1 (29,35). To test whether DPR proteins could also inhibit this import pathway, we used a second reporter (RFP-NLS$_{PY}$) containing the well characterised PY-NLS of hnRNPA1 (Supplementary Material, Fig. S1B and C). The nuclear localization of this reporter was not affected by expression of poly-GA, -GR, or -PR. Thus, DPR proteins mainly affect the nuclear import through the classical importin α/β pathway. In particular, poly-GA inclusions inhibit nuclear import of a TDP-43 NLS-containing reporter protein more severely than poly-GR.

Poly-GA inhibits nuclear import of p65

To analyse the effect of poly-GA on the importin α/β-mediated nuclear import on an endogenous protein, we investigated the nuclear translocation of the transcription factor p65 (also known as RelA or NFκB3) in response to TNFα stimulation in HeLa cells. In ~90% of the unstimulated cells expressing GFP or GA$_{149}$-GFP, p65 is restricted to the cytoplasm (Fig. 3A first and third row, quantification in Fig. 3B). Upon TNFα stimulation (4 ng/ml, 30 min), p65 translocated into the nucleus of ~80% of the cells expressing GFP (Fig. 3A, second row). In contrast, only
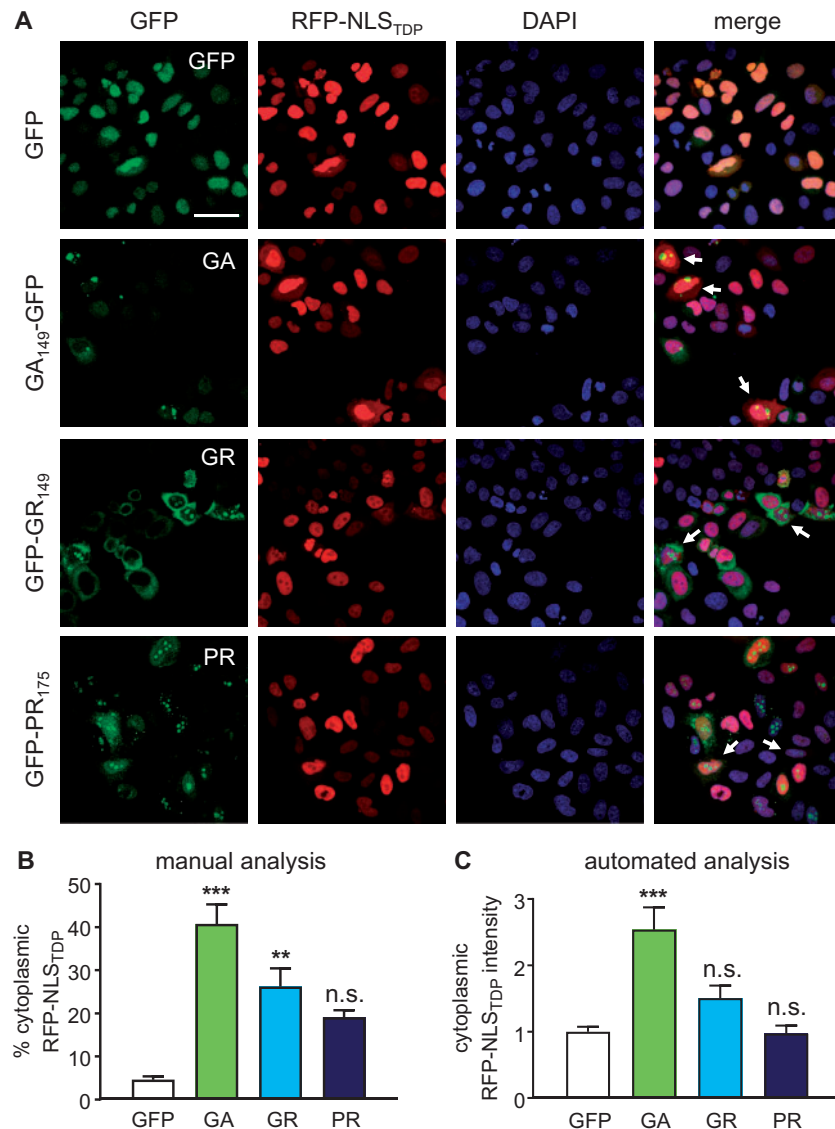
Figure 1. poly-GA reduces the activity of the TDP-43 nuclear localization signal. HeLa cells were cotransfected with RFP fused to the nuclear localization signal of TDP-43 and GFP or GFP-tagged DPR expression vectors. **(A)** Images show RFP and GFP fluorescence of cells stained with DAPI to visualise nuclei. Note that many cells with compact poly-GA inclusions (arrows) show significant levels of RFP-NLS$_{TDP}$ in the cytoplasm. **(B)** Manual quantification of the percentage of cells showing cytoplasmic mislocalization of the RFP-NLS$_{TDP}$ reporter in cells co-expressing GFP or DPR-GFP inclusions. $n = 4$–5 biological replicates, each containing 38–344 double positive cells from 3 to 6 tile scans each. Mean ± SEM. One way ANOVA with Dunnett's post-test, *** denotes $P<0.001$, * denotes $P<0.05$). Scale bar denotes 50 µm. **(C)** Automatic image analysis of reporter localization in HeLa cells coexpressing GFP or GFP-tagged DPR. The mean level of cytoplasmic of RFP-NLS$_{TDP}$ is shown. $n = 7$–8 tiles scans containing 994–2009 cells per group from 5 independent experiments. Mean ± SEM. One-way ANOVA with Dunnett's post-test, *** denotes $P<0.001$.

46% of the cells with GA$_{149}$-GFP inclusions show nuclear translocation of p65 (Fig. 3A, fourth row). Subcellular fractionation corroborates impaired nuclear import of p65 upon TNFα stimulation in poly-GA expressing cells on a biochemical level (Supplementary Material, Fig. S2). Thus, poly-GA aggregation in HeLa cells can directly inhibit nuclear import of p65 and possibly other signalling factors which may affect the function and survival of inclusion bearing neurons.

Poly-GA enhances TDP-43 localization into cytoplasmic granules in neurons

Next, we analysed how DPR aggregates affect the nuclear import in hippocampal neurons. Normally, TDP-43 is predominantly nuclear, but a small fraction of TDP-43 is found in cytoplasmic RNA transport granules (36). We expressed GFP-tagged DPR proteins using lentivirus and analysed the localization of endogenous TDP-43 in hippocampal neurons. Consistent with previous reports, none of the DPR proteins led to dramatic mislocalization or even aggregation of TDP-43 in the cytoplasm. However, poly-GA expression consistently enhanced cytoplasmic TDP-43 granules (arrows in Fig. 4A). Such cytoplasmic TDP-43 granules were present in about 80-90% of neurons expressing poly-GA, compared to ~35% in the GFP control (Fig. 4B). While poly-GR had no effect on TDP-43 localization in this assay, poly-PR expression also promoted the formation of cytoplasmic TDP-43 granules found in ~50% of the neurons. This finding was confirmed by automated analysis of the ratio of cytoplasmic to nuclear TDP-43 (Fig. 4C).
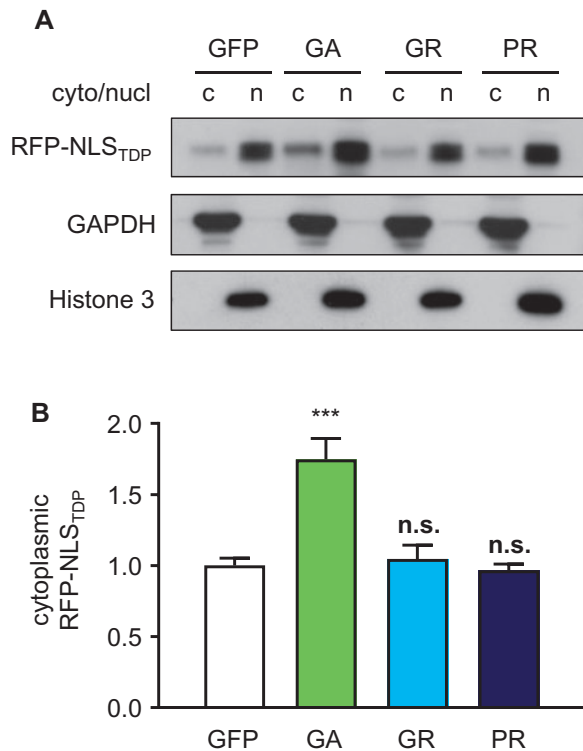
A

B

Figure 2. poly-GA induces cytoplasmic mislocalization of the RFP-NLS$_{TDP}$ reporter. HeLa cells cotransfected with RFP-NLS$_{TDP}$ and GFP or GFP-tagged DPR expression vectors were subjected to subcellular fractionation. (**A**) Immunoblot of cytoplasmic and nuclear fractions with the indicated antibodies. GAPDH and histone 3 are used as markers for cytoplasm and nucleus, respectively. (**B**) Quantification of cytoplasmic RFP-NLS$_{TDP}$ from $n=4$ biological replicates. Mean ± SEM. One way ANOVA with Dunnett's post-test, *** denotes $P<0.001$.

We noticed no significant colocalization of any DPR species with TDP-43. In order to determine the nature of the cytoplasmic TDP-43 granules in poly-GA-expressing neurons, we analysed colocalization with stress granules and lysosomes. Cytoplasmic TDP-43 partially localised in LAMP1-positive lysosomes, but not the stress granule marker TIAR (Supplementary Material, Fig. S3).

Thus, poly-GA inhibits the nuclear localization of TDP-43 in neurons consistent with the results using the RFP-NLS$_{TDP}$ reporter in HeLa cells.

Rerouting of poly-GA to the nucleus prevents cytoplasmic TDP-43 mislocalization

As artificial β-sheet proteins only inhibit nuclear import when they aggregate in the cytosol, but not in the nucleus (31), we asked whether the localization of poly-GA aggregates is critical for their effects on TDP-43 import. Thus, we fused poly-GA with the NLS of the SV40 large T antigen to shift aggregate formation from the cytosol to the nucleus.

Indeed, in neurons about 40% of the GA$_{175}$-NLS inclusions were found in the nucleus, although many cells still bore residual cytoplasmic inclusion indicating incomplete nuclear import of GA$_{175}$-NLS (Fig. 5A). While neurons with cytoplasmic GA$_{175}$-NLS aggregates often contain cytoplasmic TDP-43 granules, cells with pure nuclear GA$_{175}$-NLS aggregation showed lower level of TDP-43 mislocalization comparable to controls (Fig. 5B).

GA$_{149}$-GFP-NLS expressing HeLa cells showed less often cytoplasmic mislocalization of the RFP-NLS$_{TDP}$ reporter than GA$_{149}$-GFP expressing cells (Fig. 5C, compare Fig. 1). While 45% of cells with residual cytoplasmic GA$_{149}$-GFP-NLS aggregates showed cytoplasmic mislocalization of the RFP-NLS$_{TDP}$ reporter, only 17% of cells with GA$_{149}$-GFP-NLS inclusions restricted to the nucleus showed cytoplasmic RFP-NLS$_{TDP}$ fluorescence (Fig. 5D). Thus, only cytoplasmic poly-GA aggregates disturb nuclear import of TDP-43 similar to the findings with artificial β-sheet proteins (31).

Overexpression of importin-α and nuclear pore components restores nucleocytoplasmic transport in poly-GA expressing cells

Since (GGGGCC)$_n$ RNA and poly-GR/PR toxicity has been rescued by Ran and RanGAP1 overexpression in drosophila and yeast (26–28,37), we asked whether it would also restore nuclear import of TDP-43 in poly-GA expressing cells. However, co-transfection of Ran or RanGAP1 did not affect poly-GA induced cytoplasmic mislocalization of the RFP-NLS$_{TDP}$ reporter (Supplementary Material, Fig. S4) despite robust expression of Ran and RanGAP1 in HeLa cells (Supplementary Material, Fig. S5A). In contrast to a previous report (30), we also found no specific colocalization of poly-GA aggregates with endogenous Ran or RanGAP1 (Supplementary Material, Fig. S5B).

We therefore tested importin-α (isoforms KPNA3 and KPNA4), the cytoplasmic receptor for the TDP-43 NLS (32), and crucial factors for nuclear import of TDP-43, such as CSE1L/CAS (which helps to recycle importin-α from the nucleus to the cytoplasm after releasing its cargo) and the nuclear pore complex components NUP54 and NUP62 (32). KPNA4 and NUP62 have also been linked to nucleocytoplasmic transport deficits in various *C9orf72* model systems (26–28,37). Co-expression of these proteins in the GFP control cells partially reduced cytoplasmic localization of the RFP-NLS$_{TDP}$ reporter, however, without reaching statistical significance (Fig. 6A and B). In contrast, co-expression of these factors in GA$_{149}$-GFP transfected cells significantly reduced mislocalization of the reporter. Importantly, expression of KPNA3, NUP54 and NUP62 fully restored nuclear localization of the RFP-NLS$_{TDP}$ reporter to control levels. Thus, our data suggest that poly-GA interferes with the nuclear transport machinery without affecting the Ran-GTP gradient.

Discussion

The expanded *C9orf72* repeat RNA and arginine-rich DPR proteins poly-GR/PR have been previously linked to impaired nucleocytoplasmic transport, but surprisingly poly-GA, the most abundant DPR species, has not been analysed (26–28,37). Here we show that cytoplasmic aggregates of poly-GA inhibit nuclear import of TDP-43 to an even greater extent than poly-GR/PR. This defect is rescued by overexpression of several nuclear transport components. Our data point to a specific inhibition of the import-α/β pathway by cytoplasmic poly-GA aggregates, because rerouting poly-GA aggregates to the nucleus also restored nuclear import of TDP-43.

Poly-GA inhibits nuclear import of TDP-43

Since (GA)$_{15}$ but not 15-mers of the other DPR species adopt an amyloid conformation (14) and synthetic β-sheet proteins can inhibit nuclear transport (31), we analysed the effect of poly-GA
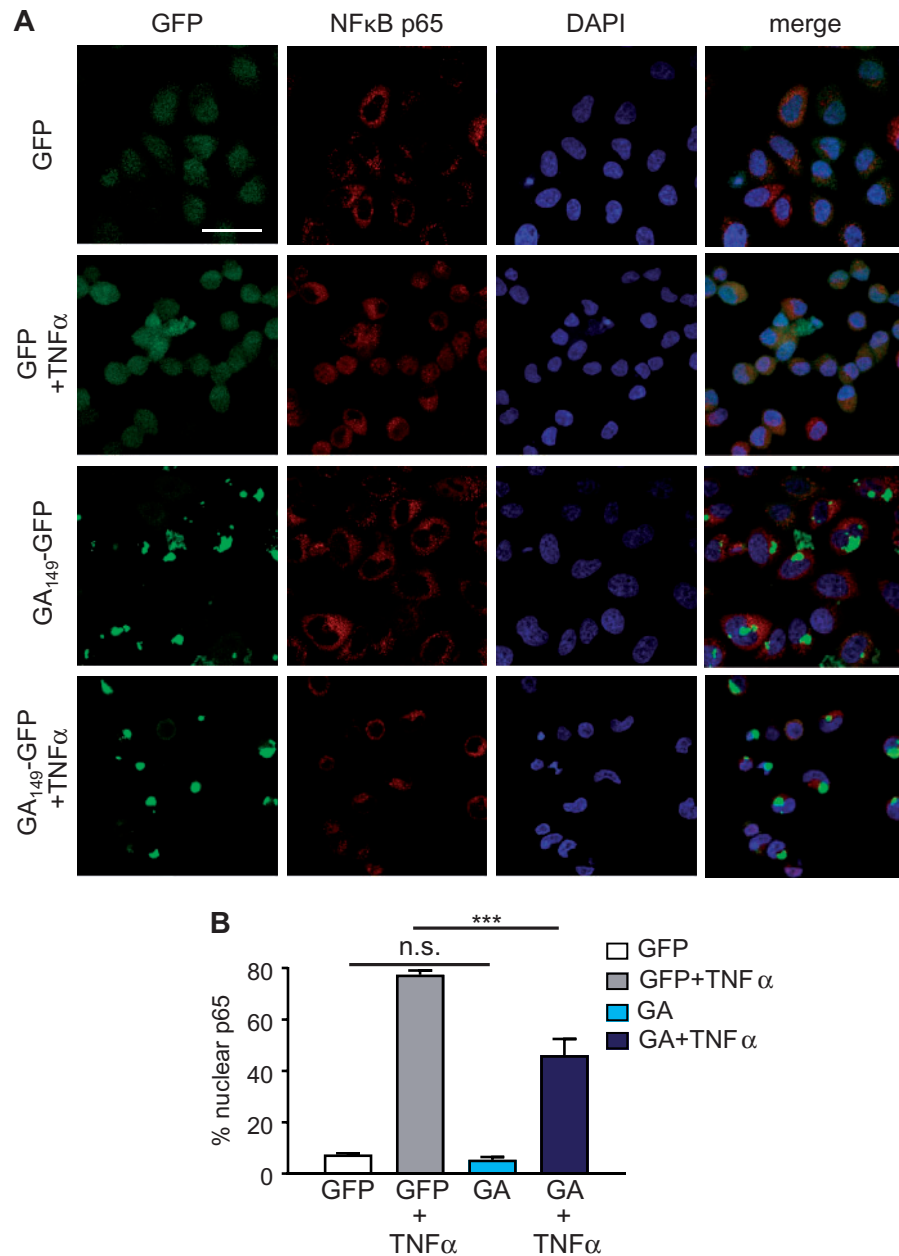
A

	GFP	NFκB p65	DAPI	merge

B

Figure 3. poly-GA inhibits nuclear import of p65. HeLa cells transfected with GFP or GA_{149}-GFP expression vectors were treated with TNFα (4 ng/ml) for 30 min to induce nuclear import of p65/RelA. **(A)** Immunofluorescence images showing p65 and GFP/GA_{149}-GFP. Nuclei were labelled with DAPI. Single confocal planes are shown. **(B)** Quantification shows the fraction of cells with nuclear p65 staining depending on the presence of diffuse or aggregated GFP or GA_{149}-GFP (n=4 experiments, each counting 66–303 double positive cells in 3–6 images, Mean ± SEM. One way ANOVA with Dunnett's post-test, *** denotes $P<0.001$, * denotes $P<0.05$). Scale bar denotes 50 μm.

on nuclear import comparing it to poly-GR and poly-PR. In contrast to the previous studies, we focused on the nuclear import of TDP-43, because the cytoplasmic mislocalization and aggregation of this nuclear RNA binding protein seem to be a crucial trigger of neurodegeneration in ALS/FTD (13,38). Poly-GA had a more dramatic effect on nuclear import of TDP-43 than poly-GR/PR in HeLa cells and in primary neurons (Figs 1 and 3). 40% of HeLa cells containing compact poly-GA inclusion showed reduced nuclear import of an RFP reporter containing the TDP-43 NLS. In primary neurons, even 80% of cells with poly-GA inclusions showed cytoplasmic TDP-43 granules compared to 35% in controls after one week of expression. While one group reported

partial colocalization of TDP-43 with cytoplasmic poly-GR and poly-PR aggregates in HEK293 cells (39), no other publication showed direct effects of the repeat RNA or individual DPR species on TDP-43 localization, phosphorylation or aggregation in cellular models (18–21). So far only two *C9orf72* models reproduced significant TDP-43 pathology, however, without elucidating the mechanism. A subset of fast progressing BAC transgenic mice showed TDP-43 aggregates in the areas of neurodegeneration (25). In the AAV-based $(GGGGCC)_{66}$ expressing mouse model TDP-43 aggregates were predominantly in neurons showing co-aggregates of poly-GA and poly-GR at 6 months of age (22). Therefore, the subtle TDP-43 mislocalization seen after
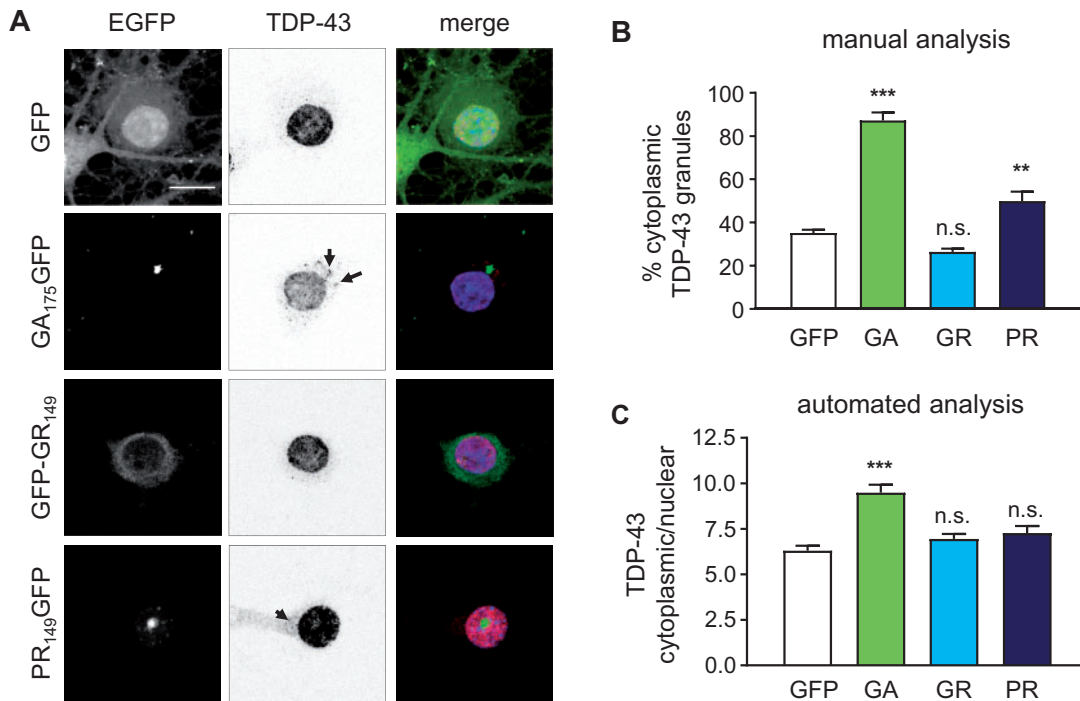
Figure 4. poly-GA inclusions induce partial TDP-43 mislocalization. Primary hippocampal neurons were transduced with GFP or GFP-tagged DPR proteins (DIV6 + 7) and endogenous TDP-43 localization was analysed by immunofluorescence. **(A)** Immunostaining shows enhanced punctate staining in the cytoplasm of neurons expressing cytoplasmic poly-GA inclusions and diffuse cytoplasmic TDP-43 mislocalization in poly-PR expressing cells. The TDP-43 panel is inverted to better visualise cytoplasmic TDP-43 granules (arrows). Scale bar denotes 15 μm. **(B)** Manual quantification of the fraction of neurons containing cytoplasmic TDP-43 granules in cells containing DPR aggregates compared to GFP control. Note that quantification was done from TDP-43 images taken under identical settings. $n = 10$ tile scans per condition with 12–51 cells per image. Mean ± SEM. One way ANOVA with Dunnett's post-test, *** denotes $P<0.001$, ** denotes $P<0.01$. **(C)** Automatic quantification of ratio of cytoplasmic to nuclear TDP-43 in GFP or GFP-DPR transduced neurons. $n = 20$-30 tile scans containing 32–80 neurons from 3 independent experiments. Mean ± SEM. One way ANOVA with Dunnett's post-test, *** denotes $P<0.001$.

1 week in our cellular poly-GA model might be a precursor for further aggregation. In primary neurons, only poly-GA and poly-PR, but not poly-GR affected TDP-43 localization, which is consistent with the weaker toxicity of poly-GR compared to poly-PR [20,27]. A potential confound is the weaker expression of poly-PR compared to poly-GA in our system. However, since poly-GA aggregates are over 100-fold more abundant than poly-PR aggregates we favour a crucial role of poly-GA in patients [40].

While none of the DPR proteins affected the localization of a reporter containing a transportin-dependent PY-NLS (Supplementary Material, Fig. S1), poly-GA also inhibited TNFα induced nuclear import of endogenous p65 in HeLa cells suggesting a broad effect on importin α/β dependent nuclear import (Fig. 2 and Supplementary Material, Fig. S2). Impaired NF-κB signalling in neurons may affect neurogenesis and synaptic plasticity [41,42]. Thus, impaired nucleocytoplasmic transport due to poly-GA cytoplasmic inclusions may have implications for *C9orf72* ALS/FTD pathogenesis beyond contributing to TDP-43 pathology.

How do DPRs affect nucleocytoplasmic transport?

Several mechanisms for impaired nucleocytoplasmic transport in *C9orf72* models have been proposed. GGGGCC RNA expressed as an exon and poly-GR/PR have been reported to disturb the Ran-GTP gradient presumably through direct binding of RanGAP1 [26]. In the repeat RNA expressing flies these effects were rescued by overexpression of Ran, RanGAP1 and importin-α [26] or components of the nuclear pore complex [28]. In contrast, intronic expression of the repeat RNA as in patients causes no toxicity in flies [43]. In yeast and flies, poly-PR toxicity can be rescued by promoting formation of the nucleocytoplasmic Ran-GTP gradient and overexpression of several importins [27,37], but the primary cause of the effect remains unknown.

We found no evidence for altered Ran localization and coaggregation of RanGAP1 with poly-GA in our cellular models (Supplementary Material, Fig. S5), while others had reported partial colocalization of poly-GA and RanGAP1 in mice [19]. In line with these findings, overexpression of Ran or RanGAP1 did not restore the impaired import of the RFP-NLS reporter in our system (Supplementary Material, Fig. S4). However, overexpression of importin-α (KPNA3), the receptor for the classical NLS of both TDP-43 and p65 [32,44], restored nuclear import mediated by the TDP-43 NLS. Moreover, overexpression of two nuclear pore components (NUP54 and NUP62) fully rescued nuclear localization of the reporter. Interestingly, NUP54 and NUP62 were previously shown to be essential for nuclear import of TDP-43 [32] and NUP62 knockdown enhances $(PR)_{25}$ toxicity in flies [37].

In patients, about 10% of poly-GA inclusions are intranuclear and their pathological relevance has been unclear [40]. We show that rerouting poly-GA aggregation into the nucleus by adding an NLS prevents the toxic effects on nuclear import suggesting that the factors responsible for the nuclear transport deficit are mainly localised in the cytoplasm. Our data are in line with the findings on synthetic β-sheet proteins [31], although their interactome is vastly different from the poly-GA interactome [18]. Cytoplasmic poly-Q aggregates inhibit nuclear
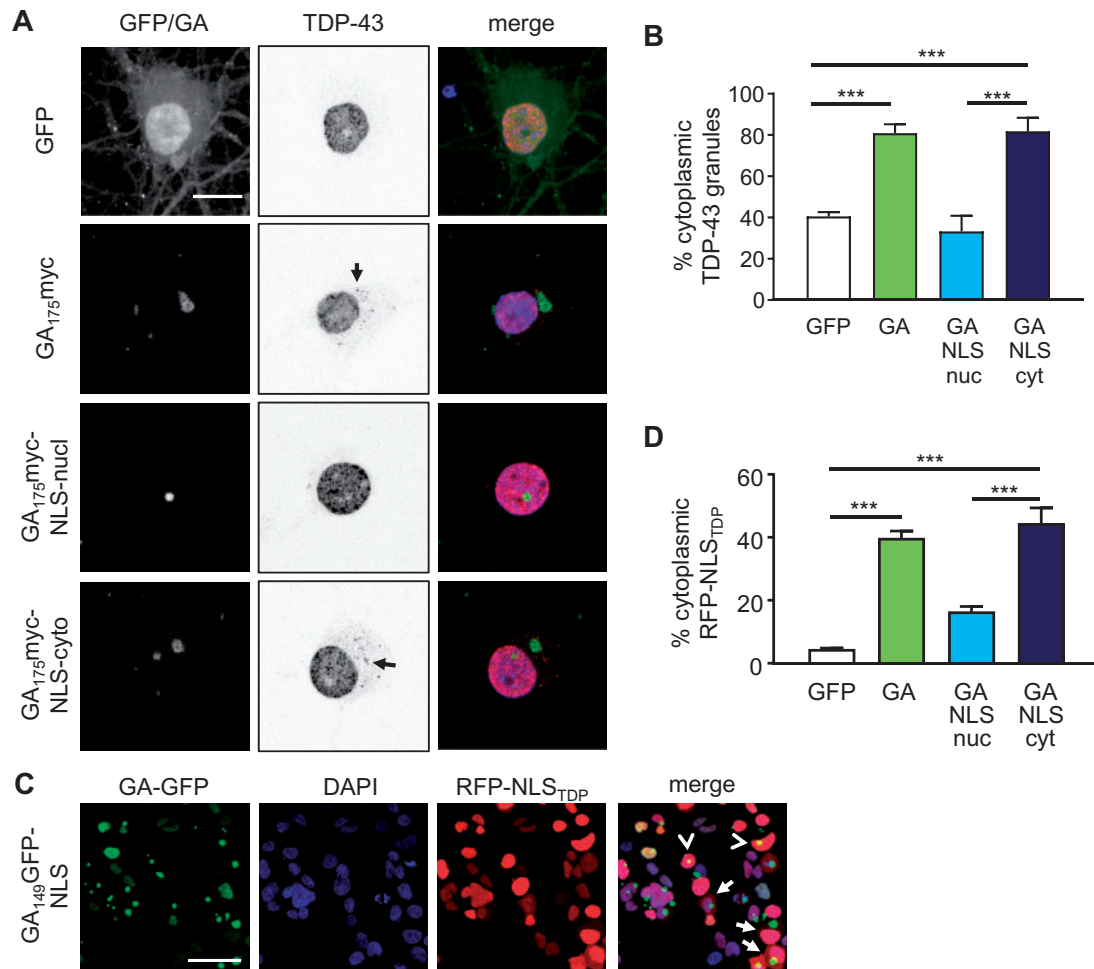
Figure 5. Only cytoplasmic poly-GA inclusions affect TDP-43 localization. **(A,B)** Primary hippocampal neurons were transduced with GFP or GA$_{175}$-myc constructs (DIV6 + 7) and endogenous TDP-43 localization was analysed by immunofluorescence. The NLS of SV40 large T was used to reroute poly-GA aggregates to the nucleus. **(A)** Immunostaining of representative cells shows partial cytoplasmic TDP-43 mislocalization (arrows). The TDP-43 panel is inverted to better visualise cytoplasmic TDP-43 granules. Scale bar denotes 15 μm. **(B)** Quantification of neurons showing cytoplasmic TDP-43 granules. GA$_{175}$-NLS transduced cells were separated according to the localization of poly-GA inclusions in the nucleus or cytoplasm ($n = 10$ tile scans per condition with 19–50 cells per image. Mean ± SEM, one way ANOVA with Dunnett's post-test, *** denotes $P < 0.001$). **(C,D)** HeLa cells were transfected with RFP-NLS together with GA$_{149}$-GFP-NLS as in Figure 1. Data was pooled from four experiments together. **(C)** Immunofluorescence showing RFP-NLS mislocalization in cells with cytoplasmic poly-GA aggregates (arrows) and reduced mislocalization in cells with nuclear poly-GA aggregates (arrowheads). Scale bar denotes 50 μm. **(D)** Quantification of RFP-NLS mislocalization from the groups in Figure 4C ($n = 4$ experiments, 27–252 double positive cells per replicate from 2 to 4 images. Mean ± SEM. One way ANOVA with Dunnett's post-test, *** denotes $P < 0.001$).

degradation of misfolded cytoplasmic proteins by sequestration of chaperones in yeast (45), suggesting that intranuclear DPR aggregates found in patients might also be targeted for degradation, while cytoplasmic aggregates inhibit nuclear import of TDP-43 and other proteins (31).

ALS/FTD with additional TDP-43 pathology (2). Our data show for the first time a direct link between poly-GA, the main aggregating protein in *C9orf72* patients, and TDP-43 mislocalization and further highlights the role of nucleocytoplasmic transport in *C9orf72* pathogenesis.

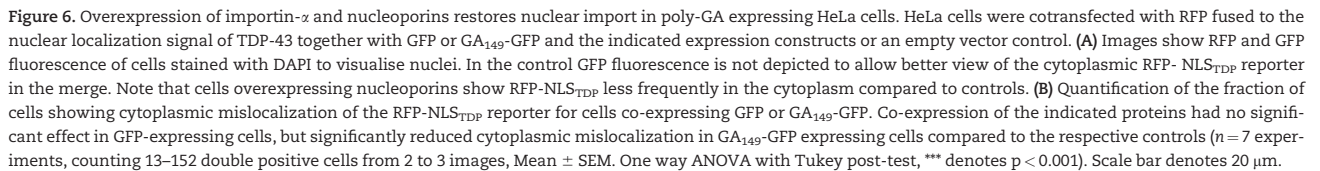### Implications for C9orf72 ALS/FTLD

Although gain-of-function mechanisms clearly trigger TDP-43 pathology and neurodegeneration in model systems (4,22,25), neither RNA foci nor any of the DPR species correlates strongly with TDP-43 pathology in patients (13,40). These data argue for synergistic effects of repeat RNA and different DPR species on TDP-43 aggregation possibly involving non-cell-autonomous effects. Two recent studies suggest that poly-GA may be transmitted between cells similar to tau and β-synuclein (14,15,46,47). These non-cell-autonomous effects may explain the slow transition from a prodromal DPR-only stage to the clinical stage of

Materials and Methods

Antibodies and reagents

TDP-43 (CAC-TIP-TD-P09, Cosmo bio Tokyo, Japan), myc (9E10, Santa Cruz Biotechnology, Dallas, TX, USA), HA (3F10, Sigma), NF-κB p65 (D14E12, Cell Signaling Technology, Danvers, MA, USA), Ran (ab53775, Abcam, Cambridge, UK), RanGAP1 (ab92360, Abcam), Anti-Histone H3 (ab10799, Abcam), LAMP1 (Ly1C6, Enzo life sciences, Farmingdale, NY, USA), TIAR (BD life sciences, Durham, NC, USA), Tumor Necrosis Factor alpha, human recombinant (rHuTNFα, 50435.50, Biomol, Hamburg, Germany),

Figure 6. Overexpression of importin-α and nucleoporins restores nuclear import in poly-GA expressing HeLa cells. HeLa cells were cotransfected with RFP fused to the nuclear localization signal of TDP-43 together with GFP or GA$_{149}$-GFP and the indicated expression constructs or an empty vector control. **(A)** Images show RFP and GFP fluorescence of cells stained with DAPI to visualise nuclei. In the control GFP fluorescence is not depicted to allow better view of the cytoplasmic RFP- NLS$_{TDP}$ reporter in the merge. Note that cells overexpressing nucleoporins show RFP-NLS$_{TDP}$ less frequently in the cytoplasm compared to controls. **(B)** Quantification of the fraction of cells showing cytoplasmic mislocalization of the RFP-NLS$_{TDP}$ reporter for cells co-expressing GFP or GA$_{149}$-GFP. Co-expression of the indicated proteins had no significant effect in GFP-expressing cells, but significantly reduced cytoplasmic mislocalization in GA$_{149}$-GFP expressing cells compared to the respective controls ($n = 7$ experiments, counting 13–152 double positive cells from 2 to 3 images, Mean ± SEM. One way ANOVA with Tukey post-test, *** denotes $p < 0.001$). Scale bar denotes 20 μm.

GAPDH (AM4300, ThermoFisher Scientific, Waltham, MA, USA). Anti-GFP (N86/8, UC Davis/NeuroMab Facility, UC Davis, CA, USA), Anti-tRFP antibody (AB233, Evrogen, Russian Federation).

Plasmids, transfection and viral packaging

Synthetic DPR constructs containing an ATG start codon for lentiviral expression (synapsin promoter) and transient transfection (EF1 promoter) were described before (18,40). Additionally, we generated tagRFP and iRFP670 tagged variants to allow multi-channel imaging. The NLS of human TDP-43

(PKDNKRKMDETDASSAVKVKRA, position 78–99) or hnRNP A1 (60 C-terminal amino acids from human) were fused to the tagRFP C-terminus. To reroute poly-GA to the nucleus, the SV40 Large T-antigen (PKKKRKV) was fused to the C-terminus of GA$_{175}$-myc and GA$_{149}$-GFP. Rescue experiments were performed using HA-tagged KPNA3, KNPA4, CSE1L, NUP54 and NUP62, Ran and RanGAP1 (cloned from human cDNA) driven by the human Ubiquitin promoter. HeLa cells were transfected with Lipofectamine 2000 (Life Technologies) for immunostaining and immunoblotting. Lentivirus was packaged in HEK293FT cells using the VSV-G/pSPAX2 system as described before (18).

Neuron culture, immunostaining and quantification

Primary hippocampal neurons were cultured from embryonic day 19 rats and infected with lentivirus as described previously (18). Transduction of the primary neurons with specified lentiviruses was performed at day 6 or 7 in vitro (DIV6/DIV7). 7 days after transduction the neurons were fixed with 4% paraformaldehyde, permeabilised (0.2% Triton X-100, 50 mM NH_4Cl in PBS) and blocked for 30 min (2% fetal bovine serum, 2% serum albumin, 0.2% fish gelatin in PBS). After 1h incubation in primary antibody solution (diluted in blocking buffer) at room temperature, coverslips were washed and finally incubated in Alexa-coupled secondary antibody solution. Heat shock was performed for 1h at 44 °C at 5% CO_2.

Fractionation

Subcellular fractionation of p65 was performed as described (48). To analyse the cytoplasmic fraction of RFP-NLS$_{TDP}$ reporter we homogenised HeLa cells in hypotonic buffer (10 mM MOPS, pH 7.0, 10 mM KCl, with protease inhibitors) using a tight fitting homogenizer (30 strokes). The nuclear fraction was pelleted by centrifugation (1,000 g for 15 min at 4 °C). Other membranous compartments were cleared from the supernatant by further centrifugation (100,000g for 1 h at 4 °C) to yield the cytoplasmic fraction.

Microscopy and image analysis

Images were taken at the confocal laser scanning microscope LSM710 from Zeiss with a Plan Apochromat oil immersion objective (40x, NA 1.4). If possible images were taken blind to the experimental condition. Most images were taken as tile scans to avoid bias for the area selection for quantification. For each experiment, data from several images were averaged. The RFP-NLS reporters and TDP-43 were imaged using identical settings for all groups. Images were manually analysed using Metamorph Software and ImageJ (version 1.49g) without intensity or size thresholding. Statistical analysis was done in GraphPad Prism (version 7.01) using one way ANOVA.

Automatic image analysis was executed with Columbus Acapella version 2.4.1 (PerkinElmer). Nucleus candidate objects were detected on the basis of the DNA stain by using "Find Nuclei C" (Area $> 30\,\mu m^2$, Split Factor: 7.0, Individual Threshold 0.4, Contrast > 0.45). Dead and mitotic nuclei were rejected by applying a linear classifier with the "Select Population" function. The classification was based on following nucleus features: Area, Roundness, Haralick Homogeneity, Haralick Correlation. The training set consisted of ∼60 manually selected nuclei across all populations. For all selected nuclei, cell region was defined by growing the nucleus region for 6 μm with morphological dilation. We selected GFP and GFP-DPR positive cells by setting a threshold on the mean intensity in the nucleus region. From this selection, RFP positive cells were selected by a second threshold on the basis of the RFP channel. We defined different thresholds for HeLa and neuronal cells. However, thresholds were kept constantly across all sub populations. For HeLa cells, we analysed the mean RFP-NLS$_{TDP}$ intensity in cytoplasm. For neurons, we quantified the mean cytoplasmic and nuclear TDP-43 intensity and determined the cytoplasmic/nuclear TDP-43 ratio for each cell. Averaged results from one image were treated as $n = 1$ for the statistical analysis.

Supplementary Material

Supplementary Material is available at *HMG* online.

References

1. Ling, S.C., Polymenidou, M. and Cleveland, D.W. (2013) Converging mechanisms in ALS and FTD: disrupted RNA and protein homeostasis. *Neuron*, **79**, 416–438.
2. Edbauer, D. and Haass, C. (2016) An amyloid-like cascade hypothesis for C9orf72 ALS/FTD. *Curr Opin Neurobiol*, **36**, 99–106.
3. O'Rourke, J.G., Bogdanik, L., Yanez, A., Lall, D., Wolf, A.J., Muhammad, A.K., Ho, R., Carmona, S., Vit, J.P., Zarrow, J., et al. (2016) C9orf72 is required for proper macrophage and microglial function in mice. *Science*, **351**, 1324–1329.
4. Jiang, J., Zhu, Q., Gendron, T.F., Saberi, S., McAlonis-Downes, M., Seelman, A., Stauffer, J.E., Jafar-Nejad, P., Drenner, K., Schulte, D., et al. (2016) Gain of Toxicity from ALS/FTD-Linked Repeat Expansions in C9ORF72 Is Alleviated by Antisense Oligonucleotides Targeting GGGGCC-Containing RNAs. *Neuron*, **90**, 535–550.
5. Farg, M.A., Sundaramoorthy, V., Sultana, J.M., Yang, S., Atkinson, R.A., Levina, V., Halloran, M.A., Gleeson, P.A., Blair, I.P., Soo, K.Y., et al. (2014) C9ORF72, implicated in amytrophic lateral sclerosis and frontotemporal dementia, regulates endosomal trafficking. *Hum Mol Genet*, **23**, 3579–3595.
6. Mori, K., Lammich, S., Mackenzie, I.R., Forne, I., Zilow, S., Kretzschmar, H., Edbauer, D., Janssens, J., Kleinberger, G., Cruts, M., et al. (2013) hnRNP A3 binds to GGGGCC repeats and is a constituent of p62-positive/TDP43-negative inclusions in the hippocampus of patients with C9orf72 mutations. *Acta Neuropathol*, **125**, 413–423.
7. Zu, T., Gibbens, B., Doty, N.S., Gomes-Pereira, M., Huguet, A., Stone, M.D., Margolis, J., Peterson, M., Markowski, T.W., Ingram, M.A., et al. (2011) Non-ATG-initiated translation directed by microsatellite expansions. *Proc Natl Acad Sci U S A*, **108**, 260–265.
8. Mori, K., Weng, S.M., Arzberger, T., May, S., Rentzsch, K., Kremmer, E., Schmid, B., Kretzschmar, H.A., Cruts, M., Van Broeckhoven, C., et al. (2013) The C9orf72 GGGGCC repeat is translated into aggregating dipeptide-repeat proteins in FTLD/ALS. *Science*, **339**, 1335–1338.
9. Ash, P.E., Bieniek, K.F., Gendron, T.F., Caulfield, T., Lin, W.L., Dejesus-Hernandez, M., van Blitterswijk, M.M., Jansen-West, K., Paul, J.W., 3rd, Rademakers, R., et al. (2013) Unconventional translation of C9ORF72 GGGGCC expansion generates insoluble polypeptides specific to c9FTD/ALS. *Neuron*, **77**, 639–646.
10. Mori, K., Arzberger, T., Grasser, F.A., Gijselinck, I., May, S., Rentzsch, K., Weng, S.M., Schludi, M.H., van der Zee, J., Cruts,

M., *et al.* (2013) Bidirectional transcripts of the expanded C9orf72 hexanucleotide repeat are translated into aggregating dipeptide repeat proteins. *Acta Neuropathol*, **126**, 881–893.

11. Zu, T., Liu, Y., Banez-Coronel, M., Reid, T., Pletnikova, O., Lewis, J., Miller, T.M., Harms, M.B., Falchook, A.E., Subramony, S.H., *et al.* (2013) RAN proteins and RNA foci from antisense transcripts in C9ORF72 ALS and frontotemporal dementia. *Proc Natl Acad Sci U S A*, **110**, E4968–E4977.

12. Proudfoot, M., Gutowski, N.J., Edbauer, D., Hilton, D.A., Stephens, M., Rankin, J. and Mackenzie, I.R. (2014) Early dipeptide repeat pathology in a frontotemporal dementia kindred with C9ORF72 mutation and intellectual disability. *Acta Neuropathol*, **127**, 451–458.

13. Mackenzie, I.R., Arzberger, T., Kremmer, E., Troost, D., Lorenzl, S., Mori, K., Weng, S.M., Haass, C., Kretzschmar, H.A., Edbauer, D., *et al.* (2013) Dipeptide repeat protein pathology in C9ORF72 mutation cases: clinico-pathological correlations. *Acta Neuropathol*, **126**, 859–879.

14. Chang, Y.J., Jeng, U.S., Chiang, Y.L., Hwang, I.S. and Chen, Y.R. (2016) The Glycine-Alanine Dipeptide Repeat from C9orf72 Hexanucleotide Expansions Forms Toxic Amyloids Possessing Cell-to-Cell Transmission Properties. *J Biol Chem*, **291**, 4903–4911.

15. Westergard, T., Jensen, B.K., Wen, X., Cai, J., Kropf, E., Iacovitti, L., Pasinelli, P. and Trotti, D. (2016) Cell-to-Cell Transmission of Dipeptide Repeat Proteins Linked to C9orf72-ALS/FTD. *Cell Rep*, **17**, 645–652.

16. Feiler, M.S., Strobel, B., Freischmidt, A., Helferich, A.M., Kappel, J., Brewer, B.M., Li, D., Thal, D.R., Walther, P., Ludolph, A.C., *et al.* (2015) TDP-43 is intercellularly transmitted across axon terminals. *J Cell Biol*, **211**, 897–911.

17. Hayes, L.R. and Rothstein, J.D. (2016) C9ORF72-ALS/FTD: Transgenic Mice Make a Come-BAC. *Neuron*, **90**, 427–431.

18. May, S., Hornburg, D., Schludi, M.H., Arzberger, T., Rentzsch, K., Schwenk, B.M., Grasser, F.A., Mori, K., Kremmer, E., Banzhaf-Strathmann, J., *et al.* (2014) C9orf72 FTLD/ALS-associated Gly-Ala dipeptide repeat proteins cause neuronal toxicity and Unc119 sequestration. *Acta Neuropathol*, **128**, 485–503.

19. Zhang, Y.J., Jansen-West, K., Xu, Y.F., Gendron, T.F., Bieniek, K.F., Lin, W.L., Sasaguri, H., Caulfield, T., Hubbard, J., Daughrity, L., *et al.* (2014) Aggregation-prone c9FTD/ALS poly(GA) RAN-translated proteins cause neurotoxicity by inducing ER stress. *Acta Neuropathol*, **128**, 505–524.

20. Wen, X., Tan, W., Westergard, T., Krishnamurthy, K., Markandaiah, S.S., Shi, Y., Lin, S., Shneider, N.A., Monaghan, J., Pandey, U.B., *et al.* (2014) Antisense Proline-Arginine RAN Dipeptides Linked to C9ORF72-ALS/FTD Form Toxic Nuclear Aggregates that Initiate In Vitro and In Vivo Neuronal Death. *Neuron*, **84**, 1213–1225.

21. Tao, Z., Wang, H., Xia, Q., Li, K., Li, K., Jiang, X., Xu, G., Wang, G. and Ying, Z. (2015) Nucleolar stress and impaired stress granule formation contribute to C9orf72 RAN translation-induced cytotoxicity. *Hum Mol Genet*, **24**, 2426–2441.

22. Chew, J., Gendron, T.F., Prudencio, M., Sasaguri, H., Zhang, Y.J., Castanedes-Casey, M., Lee, C.W., Jansen-West, K., Kurti, A., Murray, M.E., *et al.* (2015) Neurodegeneration. C9ORF72 repeat expansions in mice cause TDP-43 pathology, neuronal loss, and behavioral deficits. *Science*, **348**, 1151–1154.

23. Peters, O.M., Cabrera, G.T., Tran, H., Gendron, T.F., McKeon, J.E., Metterville, J., Weiss, A., Wightman, N., Salameh, J., Kim, J., *et al.* (2015) Human C9ORF72 Hexanucleotide Expansion Reproduces RNA Foci and Dipeptide Repeat Proteins but Not Neurodegeneration in BAC Transgenic Mice. *Neuron*, **88**, 902–909.

24. O'Rourke, J.G., Bogdanik, L., Muhammad, A.K., Gendron, T.F., Kim, K.J., Austin, A., Cady, J., Liu, E.Y., Zarrow, J., Grant, S., *et al.* (2015) C9orf72 BAC Transgenic Mice Display Typical Pathologic Features of ALS/FTD. *Neuron*, **88**, 892–901.

25. Liu, Y., Pattamatta, A., Zu, T., Reid, T., Bardhi, O., Borchelt, D.R., Yachnis, A.T. and Ranum, L.P. (2016) C9orf72 BAC Mouse Model with Motor Deficits and Neurodegenerative Features of ALS/FTD. *Neuron*, **90**, 521–534.

26. Zhang, K., Donnelly, C.J., Haeusler, A.R., Grima, J.C., Machamer, J.B., Steinwald, P., Daley, E.L., Miller, S.J., Cunningham, K.M., Vidensky, S., *et al.* (2015) The C9orf72 repeat expansion disrupts nucleocytoplasmic transport. *Nature*, **525**, 56–61.

27. Jovicic, A., Mertens, J., Boeynaems, S., Bogaert, E., Chai, N., Yamada, S.B., Paul, J.W., 3rd, Sun, S., Herdy, J.R., Bieri, G., *et al.* (2015) Modifiers of C9orf72 dipeptide repeat toxicity connect nucleocytoplasmic transport defects to FTD/ALS. *Nat Neurosci*, **18**, 1226–1229.

28. Freibaum, B.D., Lu, Y., Lopez-Gonzalez, R., Kim, N.C., Almeida, S., Lee, K.H., Badders, N., Valentine, M., Miller, B.L., Wong, P.C., *et al.* (2015) GGGGCC repeat expansion in C9orf72 compromises nucleocytoplasmic transport. *Nature*, **525**, 129–133.

29. Prpar Mihevc, S., Darovic, S., Kovanda, A., Bajc Cesnik, A., Zupunski, V. and Rogelj, B. (2016) Nuclear trafficking in amyotrophic lateral sclerosis and frontotemporal lobar degeneration. *Brain*, in press.

30. Zhang, Y.J., Gendron, T.F., Grima, J.C., Sasaguri, H., Jansen-West, K., Xu, Y.F., Katzman, R.B., Gass, J., Murray, M.E., Shinohara, M., *et al.* (2016) C9ORF72 poly(GA) aggregates sequester and impair HR23 and nucleocytoplasmic transport proteins. *Nat Neurosci*, **19**, 668–677.

31. Woerner, A.C., Frottin, F., Hornburg, D., Feng, L.R., Meissner, F., Patra, M., Tatzelt, J., Mann, M., Winklhofer, K.F., Hartl, F.U., *et al.* (2016) Cytoplasmic protein aggregates interfere with nucleocytoplasmic transport of protein and RNA. *Science*, **351**, 173–176.

32. Nishimura, A.L., Zupunski, V., Troakes, C., Kathe, C., Fratta, P., Howell, M., Gallo, J.M., Hortobagyi, T., Shaw, C.E. and Rogelj, B. (2010) Nuclear import impairment causes cytoplasmic trans-activation response DNA-binding protein accumulation and is associated with frontotemporal lobar degeneration. *Brain*, **133**, 1763–1771.

33. Winton, M.J., Igaz, L.M., Wong, M.M., Kwong, L.K., Trojanowski, J.Q. and Lee, V.M. (2008) Disturbance of nuclear and cytoplasmic TAR DNA-binding protein (TDP-43) induces disease-like redistribution, sequestration, and aggregate formation. *J Biol Chem*, **283**, 13302–13309.

34. Ayala, Y.M., Zago, P., D'Ambrogio, A., Xu, Y.F., Petrucelli, L., Buratti, E. and Baralle, F.E. (2008) Structural determinants of the cellular localization and shuttling of TDP-43. *J Cell Sci*, **121**, 3778–3785.

35. Lee, B.J., Cansizoglu, A.E., Suel, K.E., Louis, T.H., Zhang, Z. and Chook, Y.M. (2006) Rules for nuclear localization sequence recognition by karyopherin beta 2. *Cell*, **126**, 543–558.

36. Alami, N.H., Smith, R.B., Carrasco, M.A., Williams, L.A., Winborn, C.S., Han, S.S., Kiskinis, E., Winborn, B., Freibaum, B.D., Kanagaraj, A., *et al.* (2014) Axonal transport of TDP-43 mRNA granules is impaired by ALS-causing mutations. *Neuron*, **81**, 536–543.

37. Boeynaems, S., Bogaert, E., Michiels, E., Gijselinck, I., Sieben, A., Jovicic, A., De Baets, G., Scheveneels, W., Steyaert, J., Cuijt, I., *et al.* (2016) Drosophila screen connects nuclear transport genes to DPR pathology in c9ALS/FTD. *Sci Rep*, **6**, 20877.

38. Walker, A.K., Spiller, K.J., Ge, G., Zheng, A., Xu, Y., Zhou, M., Tripathy, K., Kwong, L.K., Trojanowski, J.Q. and Lee, V.M. (2015) Functional recovery in new mouse models of ALS/FTLD after clearance of pathological cytoplasmic TDP-43. *Acta Neuropathol*, **130**, 643–660.

39. Yamakawa, M., Ito, D., Honda, T., Kubo, K., Noda, M., Nakajima, K. and Suzuki, N. (2015) Characterization of the dipeptide repeat protein in the molecular pathogenesis of c9FTD/ALS. *Hum Mol Genet*, **24**, 1630–1645.

40. Schludi, M.H., May, S., Grasser, F.A., Rentzsch, K., Kremmer, E., Kupper, C., Klopstock, T., German Consortium for Frontotemporal Lobar Degeneration, Bavarian Brain Banking Alliance, Arzberger, T., and Edbauer, D. (2015) Distribution of dipeptide repeat proteins in cellular models and C9orf72 mutation cases suggests link to transcriptional silencing. *Acta Neuropathol*, **130**, 537–555.

41. Kaltschmidt, B. and Kaltschmidt, C. (2009) NF-kappaB in the nervous system. *Cold Spring Harb Perspect Biol*, **1**, a001271.

42. Snow, W.M., Stoesz, B.M., Kelly, D.M. and Albensi, B.C. (2014) Roles for NF-kappaB and gene targets of NF-kappaB in synaptic plasticity, memory, and navigation. *Mol Neurobiol*, **49**, 757–770.

43. Tran, H., Almeida, S., Moore, J., Gendron, T.F., Chalasani, U., Lu, Y., Du, X., Nickerson, J.A., Petrucelli, L., Weng, Z., *et al.* (2015) Differential Toxicity of Nuclear RNA Foci versus Dipeptide Repeat Proteins in a Drosophila Model of C9ORF72 FTD/ALS. *Neuron*, **87**, 1207–1214.

44. Zhu, J., Cynader, M.S. and Jia, W. (2015) TDP-43 Inhibits NF-kappaB Activity by Blocking p65 Nuclear Translocation. *PLoS One*, **10**, e0142296.

45. Park, S.H., Kukushkin, Y., Gupta, R., Chen, T., Konagai, A., Hipp, M.S., Hayer-Hartl, M. and Hartl, F.U. (2013) PolyQ proteins interfere with nuclear degradation of cytosolic proteins by sequestering the Sis1p chaperone. *Cell*, **154**, 134–145.

46. Chai, X., Dage, J.L. and Citron, M. (2012) Constitutive secretion of tau protein by an unconventional mechanism. *Neurobiol Dis*, **48**, 356–366.

47. Sanders, D.W., Kaufman, S.K., DeVos, S.L., Sharma, A.M., Mirbaha, H., Li, A., Barker, S.J., Foley, A.C., Thorpe, J.R., Serpell, L.C., *et al.* (2014) Distinct tau prion strains propagate in cells and mice and define different tauopathies. *Neuron*, **82**, 1271–1288.

48. Suzuki, K., Bose, P., Leong-Quong, R.Y., Fujita, D.J. and Riabowol, K. (2010) REAP: A two minute cell fractionation method. *BMC Res Notes*, **3**, 294.